

Effects of electron spiralling on the anisotropy and polarization of photon emission from an electron beam ion trap

To cite this article: M F Gu *et al* 1999 *J. Phys. B: At. Mol. Opt. Phys.* **32** 5371

View the [article online](#) for updates and enhancements.

Related content

- [Polarization properties of dielectronic satellite lines in the K-shell x-ray spectra of B-like Fe XXII](#)
A S Shlyaptseva, R C Mancini, P Neill *et al.*
- [Plasma polarization spectroscopy](#)
Takashi Fujimoto and Sergei A Kazantsev
- [Fe XVII X-Ray Spectrum](#)
G. V. Brown, P. Beiersdorfer, D. A. Liedahl *et al.*

Recent citations

- [Measurements of density dependent intensity ratios of extreme ultraviolet line emission from Fe X, XI, and XII](#)
Erina Shimizu *et al*
- [Strong higher-order resonant contributions to x-ray line polarization in hot plasmas](#)
Chintan Shah *et al*
- [Measurement of the Radiative Decay Rate and Energy of the Metastable \(2s22p51=23s1=2\)\(J=0\) Level in Fe XVII](#)
P. Beiersdorfer *et al.*

Effects of electron spiralling on the anisotropy and polarization of photon emission from an electron beam ion trap

M F Gu[†], D W Savin[†] and P Beiersdorfer[‡]

[†] Columbia Astrophysics Laboratory and Department of Physics, Columbia University, New York, NY 10027, USA

[‡] Department of Physics and Space Technology, Lawrence Livermore National Laboratory, Livermore, CA 94550, USA

Received 22 July 1999

Abstract. We present a theoretical formalism for calculating the anisotropy and polarization of photon emission due to a spiralling beam of electrons colliding with an ensemble of atoms or ions. For an axisymmetric beam with a given velocity angular distribution, the polarization and angular distribution of the resulting radiation can be characterized by the expansion coefficients of the distribution function in terms of Legendre polynomials. We present simple expressions for dipole and quadrupole radiation and apply the results to the case of an electron beam ion trap.

1. Introduction

Ions excited by collisions with a directioned beam of electrons may emit polarized light [1,2]. This fact has recently received increasing attention because of its diagnostic potential for ascertaining the existence of directional electrons in laboratory and astrophysical plasmas [3,4]. Suggestions have been made to use polarized x-ray line emission to study, for example, beam–plasma interactions in solar flares [5–9], the properties of tokamak plasmas [10], and the production of fast directional electrons in laser–matter interactions [11, 12]. Efforts are underway using electron beam ion traps (EBITs) to test the underlying atomic physics responsible for the observed polarization [13–18]. These sources use a mono-energetic electron beam to excite trapped ions, which are essentially at rest.

EBITs appear to represent ideal sources for studying the physics of ion alignment and polarized line emission. The electron flow in the beam, however, is not truly unidirectional and laminar, as the beam electrons are produced at the electron gun with a non-vanishing thermal component. The component perpendicular to the magnetic field direction causes the electrons to gyrate. Thus, instead of following the magnetic field lines along the beam direction, the beam electrons follow a helical path. The amount of energy in the direction perpendicular to the beam direction, E_{\perp} , is thought to be small [14–16], but may be a significant fraction of the total energy if the EBIT source is run at a low beam energy. Electron spiralling, thus, has a systematic effect on the polarization and anisotropy of radiation emitted from EBIT light sources, which must be estimated in the measurements [14–16].

The effects of electron spiralling on beam-induced line emission and polarization has been treated theoretically by Haug [6]. His work, however, is valid only for electric dipole transitions. Here we present a theoretical framework for estimating the effects of electron

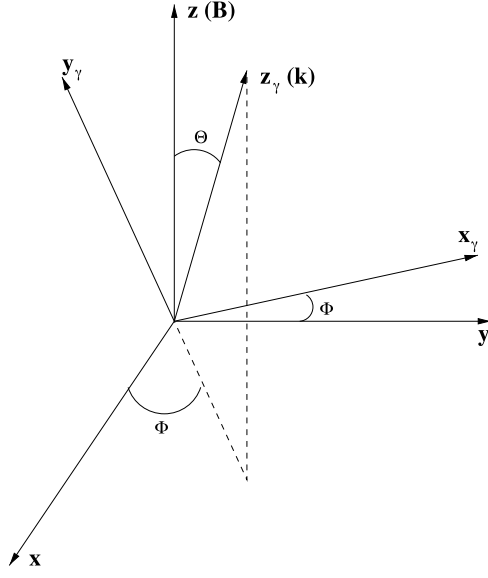


Figure 1. The relationship between the laboratory frame S and the photon frame S_γ . The projection of the z_γ -axis onto the xy -plane is shown by the dashed lines. The x_γ -axis lies in the xy -plane.

spiralling which is valid for all multipole transitions. Although including different multipole operators for a transition presents no difficulty, we will concentrate on the case where the transition can be accurately represented as being due to a single multipole operator. This is a good approximation for atomic transitions so long as $(\alpha Z_{\text{eff}})^2 \ll 1$, where α is the fine-structure constant and Z_{eff} is the effective nuclear charge of the ion [19]. Our work is based on the formalism given by Steffen and Alder [20]. The results are directly applicable to the polarization of line emission from EBIT sources. We find that simple analytical expressions can be derived to quantify the spiralling effects on the emitted radiation. These expressions can be used to assess and correct for systematic effects on line intensity and polarization measurements from such radiation sources.

2. Theory

We are interested in collision processes which form an excited ion of initial total angular momentum J_i which then radiatively decays to a final state of total angular momentum J_f . Our analysis follows the prescription of Steffen and Alder [20].

We begin by defining three reference frames: the laboratory frame, the photon frame, and the electron frame. The relationship between the three is shown in figures 1 and 2. In the laboratory frame S , \mathbf{B} defines the $+z$ -axis. In this frame, the directions of the emitted photon \mathbf{k} and of the electron velocity \mathbf{v}_e are given, respectively, by their polar angles Θ and θ , and azimuthal angles Φ and ϕ . The $+z$ -axes of the photon frame S_γ and the electron frame S_e are determined by \mathbf{k} and \mathbf{v}_e , respectively. The $+x$ -axis of S_γ is defined by $\mathbf{B} \times \mathbf{k}$. To bring S to S_γ , a rotation $R(\Phi, \Theta, \pi/2)$ is performed, where $R(\alpha, \beta, \gamma)$ is the rotation operator expressed in Euler angles [21, 22]. We define the $+x$ -axis of S_e by $\mathbf{v}_e \times \mathbf{B}$. A rotation $R(-\pi/2, \theta, \pi - \phi)$ brings S_e to S .

For radiative decays $i \rightarrow f$, the probability of detecting a photon emitted in the \mathbf{k} direction using a detector with an efficiency matrix ε is given by [20]

$$W(\mathbf{k}, \varepsilon) = \sum_{\tau, \tau'} \langle \tau | \rho_0^0(J_f) | \tau' \rangle \langle \tau' | \varepsilon | \tau \rangle (2J_f + 1)^{1/2} \quad (1)$$

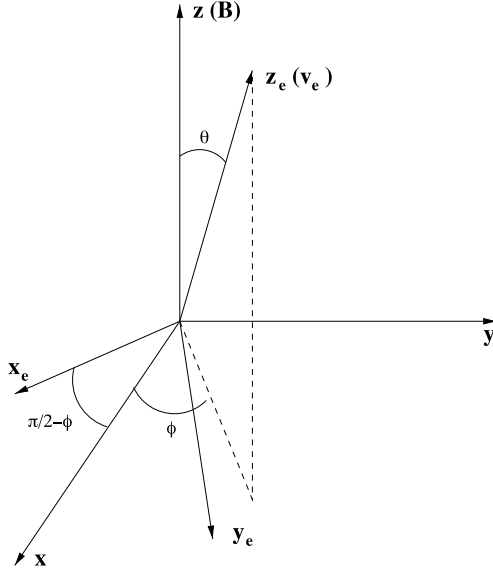


Figure 2. The relationship between the laboratory frame S and the electron frame S_e . The projection of the z_e -axis onto the xy -plane is shown by the dashed lines. The x_e -axis lies in the xy -plane.

where $\langle \tau | \rho_0^0(J_f) | \tau' \rangle$ is the reduced matrix operator in the S frame for a single photon process, $\rho_0^0(J_f)$ is a 2×2 matrix, and τ and τ' label photon helicity states. A label of τ or $\tau' = +1$ (-1) corresponds to left (right) circularly polarized light [21]. Re-expressing $\langle \tau | \rho_0^0(J_f) | \tau' \rangle$ in terms of the statistical tensor before photon emission, $\rho_q^\lambda(J_i)$, gives

$$\begin{aligned} \langle \tau | \rho_0^0(J_f) | \tau' \rangle &= \frac{d\Omega}{8\pi} \sum_{LL'\lambda q} \begin{pmatrix} L & L' & \lambda \\ \tau & -\tau' & \mu \end{pmatrix} \begin{pmatrix} 2J_i + 1 \\ 2J_f + 1 \end{pmatrix}^{1/2} \rho_q^\lambda(J_i) \\ &\quad \times [\gamma(EL) + \tau\gamma(ML)][\gamma^*(EL') + \tau'\gamma^*(ML')] \\ &\quad \times F_\lambda(LL'J_fJ_i) D_{q\mu}^{(\lambda)*}(S \rightarrow S_\gamma) \Big/ \sum_{L\pi} |\gamma(\pi L)|^2. \end{aligned} \quad (2)$$

Here $d\Omega$ is the solid angle element; L is the order of the 2^L multipole decay; the quantities in the large parenthesis denote Wigner 3- j symbols; and $\gamma(\pi L)$ is the multipole transition amplitude with $\pi = E$ (M) for electric (magnetic) transitions. $F_\lambda(LL'J_fJ_i)$ is given by

$$\begin{aligned} F_\lambda(LL'J_fJ_i) &= (-1)^{J_f+J_i-1} [(2\lambda+1)(2L+1)(2L'+1)(2J_i+1)]^{1/2} \\ &\quad \times \begin{pmatrix} L & L' & \lambda \\ 1 & -1 & 0 \end{pmatrix} \left\{ \begin{matrix} L & L' & \lambda \\ J_i & J_i & J_f \end{matrix} \right\}, \end{aligned} \quad (3)$$

where the quantity in the large braces denotes a Wigner 6- j symbol. The properties and values of the 3- j and 6- j symbols are given by Cowan [23]. $D_{q\mu}^{(\lambda)*}(S \rightarrow S_\gamma) = D_{q\mu}^{(\lambda)*}(\Phi, \Theta, \pi/2)$ is the rotation matrix from S to S_γ . The rotation matrices are described in detail in [21, 22].

Using the fact that parity is a good quantum number for atomic states, for a single multipole transition equation (2) simplifies to

$$\langle \tau | \rho_0^0(J_f) | \tau \rangle = \frac{d\Omega}{8\pi} \left(\frac{2J_i + 1}{2J_f + 1} \right)^{1/2} \sum_{\lambda q} \tau^\lambda \rho_q^\lambda(J_i) A_\lambda D_{q0}^{(\lambda)*}(S \rightarrow S_\gamma) \quad (4)$$

$$\langle \tau | \rho_0^0(J_f) | -\tau \rangle = \frac{d\Omega}{8\pi} \left(\frac{2J_i + 1}{2J_f + 1} \right)^{1/2} \sum_{\lambda q} \tau^\lambda \rho_q^\lambda(J_i) A_{\lambda,2} D_{q\mp 2}^{(\lambda)*}(S \rightarrow S_\gamma), \quad (5)$$

where $D_{q-2}^{(\lambda)*}(D_{q+2}^{(\lambda)*})$ corresponds to $\tau = +1(-1)$. $A_\lambda = F_\lambda(LLJ_fJ_i)$ and

$$A_{\lambda,2} = (-1)^{\Lambda(\pi)} \frac{\begin{pmatrix} L & L & \lambda \\ 1 & 1 & -2 \end{pmatrix}}{\begin{pmatrix} L & L & \lambda \\ 1 & -1 & 0 \end{pmatrix}} A_\lambda, \quad (6)$$

where $\Lambda(E) = 0$ and $\Lambda(M) = 1$. A_λ and $A_{\lambda,2}$ are called the angular distribution coefficients.

EBIT measurements commonly use detectors which are sensitive to linearly polarized radiation. For these detectors, the efficiency matrix in the representation of helicity states is given by [20]

$$\begin{pmatrix} \langle +1|\varepsilon|+1 \rangle & \langle +1|\varepsilon|-1 \rangle \\ \langle -1|\varepsilon|+1 \rangle & \langle -1|\varepsilon|-1 \rangle \end{pmatrix} = \frac{1}{2} \begin{pmatrix} 1 & -Qe^{-i2\alpha} \\ -Qe^{i2\alpha} & 1 \end{pmatrix}, \quad (7)$$

where Q is called the linear polarization efficiency. The detector efficiencies for radiation polarized along two orthogonal axes, p and s , are given by $\mathcal{E}_p = (1+Q)/2$ and $\mathcal{E}_s = (1-Q)/2$, respectively. α is the angle between the p -axis and the x_p -axis. In the above definition, the efficiency matrix is normalized so that the detector response to unpolarized radiation is $\frac{1}{2}$, i.e., $\mathcal{E}_p + \mathcal{E}_s = 1$. For arbitrary \mathcal{E}_p and \mathcal{E}_s , the efficiency matrix may be written as

$$\frac{1}{2} \begin{pmatrix} \mathcal{E}_s + \mathcal{E}_p & (\mathcal{E}_s - \mathcal{E}_p)e^{-i2\alpha} \\ (\mathcal{E}_s - \mathcal{E}_p)e^{i2\alpha} & \mathcal{E}_s + \mathcal{E}_p \end{pmatrix}. \quad (8)$$

The resulting angular distribution detection factor is then

$$\begin{aligned} W(\Phi, \Theta, \alpha, \mathcal{E}_p, \mathcal{E}_s) &= \frac{d\Omega}{16\pi} \sum_{\lambda q} (2J_i + 1)^{1/2} \rho_q^\lambda(J_i) \\ &\times \left\{ (\mathcal{E}_p + \mathcal{E}_s)(A_\lambda + (-1)^\lambda A_\lambda) \left(\frac{4\pi}{2\lambda + 1} \right)^{1/2} Y_{\lambda q}^*(\Theta, \Phi) \right. \\ &- (\mathcal{E}_p - \mathcal{E}_s)[A_{\lambda,2} D_{q-2}^{(\lambda)*}(\Phi, \Theta, \pi/2 + \alpha) \\ &\left. + (-1)^\lambda A_{\lambda,2} D_{q2}^{(\lambda)*}(\Phi, \Theta, \pi/2 + \alpha)] \right\}. \quad (9) \end{aligned}$$

Here we have used [22]

$$D_{q0}^{(\lambda)*}(\Phi, \Theta, \pi/2) = \left(\frac{4\pi}{2\lambda + 1} \right)^{1/2} Y_{\lambda q}^*(\Theta, \Phi), \quad (10)$$

where $Y_{\lambda q}$ is the spherical harmonic and

$$D_{q\pm 2}^{(\lambda)*}(\Phi, \Theta, \pi/2 + \alpha) = D_{q\pm 2}^{(\lambda)*}(\Phi, \Theta, \pi/2) e^{\pm i2\alpha}. \quad (11)$$

The radiating system is formed by an electron colliding with a quasistationary ion. In the S_e frame, the system is axisymmetric along v_e and the initial statistical tensor ρ_q^{λ} is nonzero only for $q = 0$ [20]. The statistical tensors in S and S_e are related by the rotation

$$\begin{aligned} \rho_q^\lambda(J_i, \theta, \phi) &= \sum_{q'} \rho_{q'}^{\lambda}(J_i) D_{q'q}^{(\lambda)*}(-\pi/2, \theta, \pi - \phi) \\ &= \rho_0^\lambda(J_i) D_{0q}^{(\lambda)*}(-\pi/2, \theta, \pi - \phi), \end{aligned} \quad (12)$$

where

$$\rho_0^\lambda(J_i) = \sum_m (-1)^{J_i+m} (2\lambda + 1)^{1/2} \begin{pmatrix} J_i & J_i & \lambda \\ -m & m & 0 \end{pmatrix} \sigma_m. \quad (13)$$

The factor σ_m represents the population density of the magnetic sublevel m . The m values are quantized along v_e . The density matrix ρ' is normalized so that $\text{Tr } \rho' = \sum_m \sigma_m = 1$. It is convenient to introduce the orientation parameters which are defined as

$$B_\lambda(J_i) = (2J_i + 1)^{1/2} \rho_0'^\lambda(J_i). \quad (14)$$

The electrons in an EBIT can be described by a pitch angle distribution $f(\cos \theta)$, which we normalize so that $\int_{-1}^1 d(\cos \theta) f(\cos \theta) = 1$. In the Lawrence Livermore EBIT and SuperEBIT [24–26], the electrons travel along the ~ 3 T magnetic field lines in the trapping volume, spiralling with a cyclotron frequency of $\sim 5.3 \times 10^{11}$ revolutions s^{-1} . For kinetic energies $\lesssim 100$ keV, the electrons undergo $\gtrsim 25$ revolutions as they traverse the observed central 1 cm length of the trap. This large number of revolutions allows us to calculate the initial statistical tensor of the radiating system by averaging equation (12) over θ and ϕ . This gives

$$\begin{aligned} \rho_q^\lambda(J_i) &= \int_{-1}^1 d(\cos \theta) f(\cos \theta) \int_0^{2\pi} \frac{d\phi}{2\pi} \rho_q^\lambda(J_i, \theta, \phi) \\ &= \rho_0'^\lambda(J_i) \int_{-1}^1 d(\cos \theta) f(\cos \theta) \int_0^{2\pi} \frac{d\phi}{2\pi} D_{0q}^{(\lambda)*}(-\pi/2, \theta, \pi - \phi) \\ &= \delta_{q0} g_\lambda \rho_q'^\lambda(J_i), \end{aligned} \quad (15)$$

where

$$g_\lambda = \int_{-1}^1 d(\cos \theta) f(\cos \theta) P_\lambda(\cos \theta), \quad (16)$$

and $P_\lambda(\cos \theta)$ is the Legendre polynomial. Using equations (9), (14) and (15) yields the angular distribution factor for radiation produced by a spiralling beam of electrons,

$$\begin{aligned} W(\Phi, \Theta, \alpha, \mathcal{E}_p, \mathcal{E}_s) &= \frac{d\Omega}{16\pi} \sum_\lambda g_\lambda B_\lambda \{ (\mathcal{E}_p + \mathcal{E}_s) (A_\lambda + (-1)^\lambda A_\lambda) P_\lambda(\cos \Theta) - (\mathcal{E}_p - \mathcal{E}_s) \\ &\quad \times [A_{\lambda,2} D_{0-2}^{(\lambda)*}(\Phi, \Theta, \pi/2 + \alpha) + (-1)^\lambda A_{\lambda,2} D_{02}^{(\lambda)*}(\Phi, \Theta, \pi/2 + \alpha)] \}. \end{aligned} \quad (17)$$

Here we have used

$$\left(\frac{4\pi}{2\lambda + 1} \right)^{1/2} Y_{\lambda 0}^*(\Theta, \Phi) = P_\lambda(\cos \Theta). \quad (18)$$

The rotation matrix elements $D_{0\pm 2}^{(\lambda)*}$ can be expressed as [22, 27]

$$D_{0\pm 2}^{(\lambda)*}(\Phi, \Theta, \pi/2 + \alpha) = - \left(\frac{(\lambda - 2)!}{(\lambda + 2)!} \right)^{1/2} P_\lambda^{(2)}(\cos \Theta) e^{\mp i 2\alpha} \quad (19)$$

where $P_\lambda^{(2)}(\cos \Theta)$ is the associated Legendre polynomial. Using equations (17) and (19) gives

$$\begin{aligned} W(\Theta, \alpha, \mathcal{E}_p, \mathcal{E}_s) &= \frac{d\Omega}{8\pi} \sum_{\lambda=\text{even}} g_\lambda A_\lambda B_\lambda [(\mathcal{E}_p + \mathcal{E}_s) P_\lambda(\cos \Theta) \\ &\quad - (\mathcal{E}_p - \mathcal{E}_s) f_\lambda(L) P_\lambda^{(2)}(\cos \Theta) \cos 2\alpha] \end{aligned} \quad (20)$$

where

$$f_\lambda(L) = -(-1)^{\Lambda(\pi)} \left(\frac{(\lambda - 2)!}{(\lambda + 2)!} \right)^{1/2} \frac{\begin{pmatrix} L & L & \lambda \\ 1 & 1 & -2 \end{pmatrix}}{\begin{pmatrix} L & L & \lambda \\ 1 & -1 & 0 \end{pmatrix}}. \quad (21)$$

Taking $\mathcal{E}_p(\mathcal{E}_s) = 1$ (0) and $\mathcal{E}_p(\mathcal{E}_s) = 0$ (1), the emitted angular distribution along the p and s axes of the detector, is given, respectively, by

$$W_{p(s)}(\Theta, \alpha) = \frac{d\Omega}{8\pi} \sum_{\lambda=\text{even}} g_\lambda A_\lambda B_\lambda [P_\lambda(\cos \Theta) \mp f_\lambda(L) P_\lambda^{(2)}(\cos \Theta) \cos 2\alpha], \quad (22)$$

where the $-$ ($+$) corresponds to the p (s) polarization component of the radiation. The polarization factor $P(\Theta, \alpha)$ can be defined as

$$\begin{aligned} P(\Theta, \alpha) &= \frac{W_s(\Theta, \alpha) - W_p(\Theta, \alpha)}{W_s(\Theta, \alpha) + W_p(\Theta, \alpha)} \\ &= \cos 2\alpha \frac{\sum_{\lambda=\text{even}} f_\lambda(L) P_\lambda^{(2)}(\cos \Theta) g_\lambda A_\lambda B_\lambda}{\sum_{\lambda=\text{even}} P_\lambda(\cos \Theta) g_\lambda A_\lambda B_\lambda}. \end{aligned} \quad (23)$$

For a non-spiralling beam with $\Theta = \pi/2$ and $\alpha = 0$, this agrees with the standard definition of the polarization factor [1, 2, 7]. Equation (20) can now be expressed in terms of $P(\Theta, \alpha)$ as

$$W(\Theta, \alpha, \mathcal{E}_p, \mathcal{E}_s) = \frac{d\Omega}{8\pi} [(\mathcal{E}_s + \mathcal{E}_p) + (\mathcal{E}_s - \mathcal{E}_p)P(\Theta, \alpha)] \sum_{\lambda=\text{even}} P_\lambda(\cos \Theta) g_\lambda A_\lambda B_\lambda. \quad (24)$$

For a polarization insensitive detector, $\mathcal{E}_p = \mathcal{E}_s = 1$, and

$$W(\Theta) = \frac{d\Omega}{4\pi} \sum_{\lambda=\text{even}} g_\lambda A_\lambda B_\lambda P_\lambda(\cos \Theta). \quad (25)$$

The upper level in the $i \rightarrow f$ decay may sometimes be populated by cascades from a higher-lying excited level. The effect of cascades on the polarization is calculated through the use of the de-orientation factor as described by Steffen and Alder [20] and applied to atomic transitions by Beiersdorfer *et al* [15]. This factor is unaffected by electron spiralling.

3. Applications

The vast majority of EBIT measurements involve the detection of dipole radiation using photon detectors placed so that $\Theta = \pi/2$ and $\alpha = 0$. For this situation

$$P = \frac{\mp 3g_2 A_2 B_2}{2 - g_2 A_2 B_2}. \quad (26)$$

Here we have used $g_0 = A_0 = B_0 = 1$ and $f_2(1) = \mp \frac{1}{2}$ where the top (bottom) sign corresponds to E1 (M1) transitions. We define $P = \mathcal{P}$ for situations where the pitch angle of the electrons $\theta = 0$, i.e., $f(\cos \theta) = \delta(\cos \theta - 1)$. Then $g_\lambda = 1$ and

$$\mathcal{P} = \frac{\mp 3A_2 B_2}{2 - A_2 B_2}. \quad (27)$$

P can now be expressed in terms of \mathcal{P} as

$$P = \mathcal{P} \frac{3g_2}{3 \mp (1 - g_2)\mathcal{P}}. \quad (28)$$

Solving equation (26) for $A_2 B_2$, the angular factor can be expressed by

$$W(\mathcal{E}_p, \mathcal{E}_s) = \frac{d\Omega}{8\pi} [(\mathcal{E}_s + \mathcal{E}_p) + (\mathcal{E}_s - \mathcal{E}_p)P] \frac{3}{3 \mp P}. \quad (29)$$

Although one seldom needs to go to higher multipoles, quadrupole transitions are sometimes important. In this case, the polarization for $f(\cos \theta) = \delta(\cos \theta - 1)$ alone does not

determine the angular distribution completely. Introducing $\beta = A_4 B_4 / A_2 B_2$ and noting that $f_2(2) = \pm \frac{1}{2}$ and $f_4(2) = \mp \frac{1}{12}$, we find

$$P = \frac{\pm(12g_2 + 5g_4\beta)A_2 B_2}{8 - (4g_2 - 3g_4\beta)A_2 B_2}, \quad (30)$$

where the top (bottom) sign corresponds to E2 (M2) transitions. The polarization for $f(\cos \theta) = \delta(\cos \theta - 1)$ is

$$\mathcal{P} = \frac{\pm(12 + 5\beta)A_2 B_2}{8 - (4 - 3\beta)A_2 B_2}. \quad (31)$$

In terms of \mathcal{P} , we have

$$P = \mathcal{P} \frac{12g_2 + 5g_4\beta}{12 + 5\beta \pm [4(1 - g_2) - 3(1 - g_4)\beta]\mathcal{P}}, \quad (32)$$

and the angular factor becomes

$$W(\mathcal{E}_p, \mathcal{E}_s) = \frac{d\Omega}{8\pi} [(\mathcal{E}_s + \mathcal{E}_p) + (\mathcal{E}_s - \mathcal{E}_p)P] \frac{12g_2 + 5g_4\beta}{12g_2 + 5g_4\beta \pm (4g_2 - 3g_4\beta)P}. \quad (33)$$

In certain circumstances, $B_4 \ll B_2$ and β is very small. An important example of this is the M2 $1s2p\ ^3P_2-1s^2\ ^1S_0$ transition produced by the electron impact excitation of He-like systems, for which, $\beta \lesssim 10^{-3}$ [15]. For cases where one can neglect terms involving β , the polarization and angular distribution of E2 (M2) transitions behave as M1 (E1) transitions.

The electron spiralling in an EBIT is commonly characterized by a typical transverse energy E_\perp , or a typical pitch angle θ_0 with $\epsilon = \sin^2 \theta_0 = E_\perp / E$, where E is the total beam energy. In this case, $f(\cos \theta) = \delta(\cos \theta - \cos \theta_0)$, and

$$\begin{aligned} g_2 &= 1 - \frac{3}{2}\epsilon, \\ g_4 &= 1 - 5\epsilon + \frac{35}{8}\epsilon^2. \end{aligned} \quad (34)$$

Therefore equations (28) and (32) become

$$P = \mathcal{P} \frac{2 - 3\epsilon}{2 \mp \epsilon \mathcal{P}}, \quad (35)$$

and

$$P = \mathcal{P} \frac{12 + 5\beta - (18 + 25\beta)\epsilon + \frac{175}{8}\epsilon^2\beta}{12 + 5\beta \pm (6\epsilon - 15\epsilon\beta + \frac{105}{8}\epsilon^2\beta)\mathcal{P}}. \quad (36)$$

4. Conclusions

The polarization and anisotropy of radiation from atoms or ions due to collisions with an axisymmetric electron beam of arbitrary velocity angular distribution can be characterized by g_λ , the expansion coefficients of the distribution function in terms of Legendre polynomials. For dipole and quadrupole transitions, simple expressions are given explicitly relating the polarization due to a spiralling beam to that due to a unidirectional one. Using these expressions adjustments can be made to the expected line polarization caused by electron spiralling that are more accurate than the previous estimates. For example, the depolarization caused by a thermal electron energy of 110 eV was estimated by Beiersdorfer *et al* [15] to reduce the measured polarization of the resonance transition in helium-like Fe^{24+} by 0.7% at a beam energy of 6.8 keV. Using our expressions we find a reduction of 1.1%. The depolarization effect will be more pronounced at lower beam energies. In the case of helium-like Ne^{8+} , the reduction will be 16% assuming the same thermal electron energy and a 1 keV beam energy. Our expressions also allow an estimate of the uncertainty introduced if no such adjustments are made, thus increasing the reliability of all atomic cross section measurements that depend on accurate line intensity measurements.

Acknowledgments

The authors wish to thank J Dubau, V L Jacobs and R E Marrs for stimulating conversation. Work at Lawrence Livermore National Laboratory was performed under auspices of the US Department of Energy (contract W-7405-ENG-48). This programme is supported by NASA High Energy Astrophysics X-Ray Astronomy Research and Analysis grant NAG5-5123 (Columbia University) and work order W-19127 (Lawrence Livermore).

References

- [1] Percival I C and Seaton M J 1958 *Phil. Trans. R. Soc. A* **251** 113
- [2] Fano U and Macek J H 1973 *Rev. Mod. Phys.* **45** 553
- [3] Kazantsev S A and Hénoux J-C 1995 *Polarization Spectroscopy of Ionized Gases* (Dordrecht: Kluwer)
- [4] Fujimoto T and Kazantsev S A 1997 *Plasma Phys. Control. Fusion* **39** 1267
- [5] Haug E 1972 *Sol. Phys.* **25** 425
- [6] Haug E 1981 *Sol. Phys.* **71** 77
- [7] Inal M K and Dubau J 1987 *J. Phys. B: At. Mol. Phys.* **20** 4221
- [8] Zhitnik I A, Korneev V V, Krutov V V, Oparin S N and Urnov A M 1988 *X-Ray Plasma Spectroscopy and the Properties of Multiply-Charged Ions* ed I I Sobel'man (Commack, NY: Nova Science)
- [9] Inal M K and Dubau J 1989 *J. Phys. B: At. Mol. Opt. Phys.* **22** 3329
- [10] Fujimoto T, Sahara H, Kawachi T, Kallstenius T, Goto M, Kawase H, Furukubo T, Maekawa T and Yerumichi Y 1996 *Phys. Rev. E* **54** R2240
- [11] Kieffer J C, Matte J P, Chaker M, Beaudoin Y, Chien C Y, Coe S, Mourou G, Dubau J and Inal M K 1993 *Phys. Rev. E* **48** 4648
- [12] Hasegawa N, Nagawa H, Youeda H, Ueda K and Takuma H 1996 *Laser Interactions and Related Phenomena (AIP Conf. Proc. No 369)* ed S Nakai and G H Miley (New York: AIP) p 660
- [13] Shlyaptseva A S, Mancini R C, Neill P and Beiersdorfer P 1997 *Rev. Sci. Instrum.* **68** 1095
- [14] Henderson J R et al 1990 *Phys. Rev. Lett.* **65** 705
- [15] Beiersdorfer P, Vogel D A, Reed K J, Decaux V, Scofield J H, Widmann K, Hölzer G, Förster E, Wehrhan O, Savin D W and Schweikhard L 1996 *Phys. Rev. A* **53** 3974
- [16] Takács E, Meyer E S, Gillaspay J D, Roberts J R, Chandler C T, Hudson L T, Deslattes R D, Brown C M, Laming J M, Dubau J and Inal M K 1996 *Phys. Rev. A* **54** 1342
- [17] Beiersdorfer P, Crespo López-Urrutia J, Decaux V, Widmann K and Neill P 1997 *Rev. Sci. Instrum.* **68** 1073
- [18] Shlyaptseva A S, Mancini R C, Neill P, Beiersdorfer P, Crespo López-Urrutia J and Widmann K 1998 *Phys. Rev. A* **57** 888
- [19] Jackson J D 1975 *Classical Electrodynamics* (New York: Wiley) p 760
- [20] Steffen R M and Alder K 1975 *The Electromagnetic Interaction in Nuclear Spectroscopy* ed W D Hamilton (New York: North-Holland) p 505
- [21] Alder K and Steffen R M 1975 *The Electromagnetic Interaction in Nuclear Spectroscopy* ed W D Hamilton (Amsterdam: North-Holland) p 1
- [22] Bohr A and Mottelson B R 1969 *Nuclear Structure* vol I (New York: Benjamin)
- [23] Cowan R D 1981 *The Theory of Atomic Structure and Spectra* (Berkeley, CA: University of California Press)
- [24] Levine M A, Marrs R E, Henderson J R, Knapp D A and Schneider M B 1988 *Phys. Scr. T* **22** 157
- [25] Levine M A et al 1989 *Nucl. Instrum. Methods B* **43** 431
- [26] Marrs R E 1995 *Experimental Methods in the Physical Sciences, Volume 29A, Atomic Molecular and Optical Physics: Charged Particles* ed F B Dunning and R G Hulet (San Diego, CA: Academic) p 391
- [27] Edmonds A R 1960 *Angular Momentum in Quantum Mechanics* (Princeton, NJ: Princeton University Press) pp 23, 24 and 59